Current Sheet Axial Dynamics of 2.5 kJ KSU-DPF under High Pressure Regime

Amgad E. Mohamed, *Member, IEEE*, Ali E. Abdou, *Member, IEEE*, Mohamed I. Ismail, *Member, IEEE,* S. Lee, S.H. Saw

***Abstract*—In Dense Plasma Focus (DPF) machines, the High pressure regime of operation can be used as alternative technique to short-circuit test as the current sheet motion is minimal. The short circuit test was performed to get the right values for the static parameters of the machine. High pressure shots of more than 30 mbar were performed on the 2.5 kJ Kansas State University Dense Plasma Focus KSU-DPF machine to determine the deviation of HP values from short circuit values in computed static inductance and resistance. The test was performed using various gases over a wide range of molecular/atomic mass, starting from hydrogen as the lightest gas up to argon. It was found that the deviation in static inductance and resistance computed from high pressure method is inversely proportional to gas molecular mass at a certain pressure. The heavy gases like neon and argon were found to give the most accurate results. At 60 mbar of argon the inductance deviation was 6.5%, and 14% for resistance. It was found also that increasing of gas pressure over 30 mbar using heavy gases like Ar or Ne gives no effective improvement of the computed static impedance. Snowplow model was used to predict the axial position and the axial speed of the current sheet during the high pressure regime. The model showed that the average axial speed in heavy gases like argon was 0.8 cm/μs, whereas in hydrogen, it was 1.6 cm/μs.**

***Index Terms*— plasma focus, high pressure discharge, static inductance, plasma resistance, axial speed, snowplow model**

I. Introduction

THE static impedance of the DPF capacitor bank is considered an important parameter in determining the behavior of the current waveform supplied to the machine. Hence, it affects the neutron yield and x-ray emission of such machine [1],[2].The plasma focus machines of Mather-type have been recently classified into two types according to the value of their static inductance [3]. The most reliable method to determine the DPF static parameters C_o, L_o, and R_o is the short circuit (SC) test. On the other hand the SC test is technically difficult to perform specially in high current machines, so it may be preferred to perform a high pressure (HP) test to get approximate values for the static parameters [4]. The assumption is that: at high pressures, the current sheet hardly moves as the high gas density suppresses the current sheet motion; the gas density in the high pressure regime is about 5 to 30 times more than the optimum gas work density.

The discharge current predominantly goes through diffusive ohmic regime rather than electromagnetic regime.

Although the high pressure gas greatly slows down the motion of the current sheet, a small displacement still exists, which adds an amount of inductance and resistance to the circuit; thus causing an over-estimation of the static parameters [1].

Manuscript received October 12, 2011.

This work was funded by the department of mechanical and nuclear engineering, Kansas State University, USA.

Amgad E. Mohamed, department of mechanical and nuclear engineering, Kansas State University, Manhattan, KS 66506 USA (email-engaesm@ksu.edu).

Ali .E. Abdou, department of mechanical and nuclear engineering, Kansas State University, Manhattan, KS 66506 USA (corresponding author, phone: 503-724-9000; fax: 785-532-7075; e-mail: aeabdou@ k-state.edu).

Mohamed .I. Ismail, department of mechanical and nuclear engineering, Kansas State University, Manhattan, KS 66506 USA (email-mismail1@ksu.edu).

S. Lee, INTI International University, 71800 Nilai, Malaysia, Institute for Plasma Focus Studies, Melbourne, Australia (e-mail: leesing@optusnet .com.au).

S. H. Saw, INTI International University, 71800 Nilai, Malaysia Institute for Plasma Focus Studies, Melbourne, Australia (e-mail: (sorheoh.saw@ newinti.edu).

II. The KSU-DPF experiment

A. KSU-DPF Specifications

The KSU-DPF is a Mather type geometry composed of three main parts: the capacitor bank comprises an Aerovox capacitor of 12.5 μF capacitance with rated voltage 20 kV and stored energy 2.5 kJ. The capacitor is charged using a General Atomics GA power supply with rated voltage 30 kV and 8 kJ/s. The capacitor is connected to the electrodes through a thyratron TDI1-200k/25kV, 10 ns jitter.

The central anode is a semi-hollow copper rod with 100mm active length and outer diameter 15 mm. The anode is surrounded by a squirrel cage cathode made of 6 equally spaced rods at a distance 29mm from the center of anode. The anode base is insulated from the cathode using a Pyrex tube of 68 mm length and 1.6 mm wall thickness. Both cathode and anode are mounted inside a stainless steel chamber with two glass windows.

The current is measured using a Rogowski coil in the *dI/dt* mode, and then numerically integrated to obtain the current waveform. A Northstar high voltage probe HV5 60/100 kV DC/AC 80 MHz was used to measure the voltage waveform across the tube.

B. Rogowski Coil Considerations

The discharge current waveform obtained from the numerically integrated Rogowski coil signal shows baseline

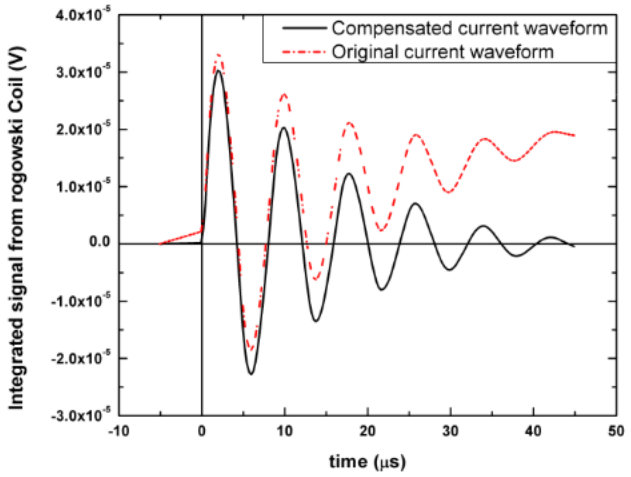

Fig. 1. Rogowski coil integrated signal, with and without compensation.

shift as shown in Fig. 1. Electromagnetic pickup, and power lines interference are potential root causes of the baseline shift [5]; the offset could also result from grounding problems or non-symmetrical topology effects with the mounting of the coil so that the coil not only monitors the current passes inside, but also the current passes outside the coil [6].

Three numerical methods were introduced to resolve the problem. The first method uses a combination of digital filters on the original *dI/dt* coil signal. Origin program was used to perform such processing.

The second method is to find the average of the signal envelope; this technique was performed by fitting the positive peaks of the waveform as well as the negative peaks then calculating the average of both fitted curves. Afterwards, this average curve was subtracted from the original waveform. The third method was performed by capturing the first few microseconds before the signal rise, and the final few microseconds close to the end of the damped curve. The time space in between the two portions was interpolated, the interpolated curve represents the base shift. Hence it was subtracted from the original waveform to obtain the compensated current without the baseline shift. The first and last method gave better prediction to the baseline shift; Fig. 1 indicates the original and the compensated curves using the first method.

C. *High Pressure Regime*

The optimum working pressure for KSU-DPF machine is about 4mbar in deuterium and 2 mbar for neon. The high pressure regime was performed under pressure range 30 - 60 mbar. The capacitor is charged to 17 kV. The working gases were argon, neon, helium, deuterium, and hydrogen.

The current waveform was measured using Rogowski coil then analyzed using the RLC analysis [1]. The resulting values for the inductance and resistance incorporate contributions due to the motion of the current sheet.

This motion has a dependence on the pressure and gas molecular weight. By studying the results in the various gases this extraneous contribution may be more readily understood and eliminated.

III. EXPERIMENTAL WORK

A short circuit test was performed first to find the static parameters of the machine. A special connector was machined with a diameter and length equal to the anode base. The connector was used to connect the anode and cathode plates, and compensate the impedance change due to removal of the real anode and cathode.

High pressure tests were performed to determine the machine static parameters; the original anode and cathode were returned back during the test. The chamber was filled with various gases at pressures from 30-60 mbar with 10 mbar increment step. A fast response Rogowski coil was fabricated to pick up the current signal. The capacitor was charged every shot to 17 kV, and then the shot was performed by turning on the thyratron switch. The current then flowed from the anode to the cathode through the gas medium in between. The experiment was repeated three times at each pressure to avoid inconsistent shots.

IV. THEORETICAL MODEL

The snowplow model was used to simulate the motion of the current sheet during the axial phase and to calculate the inductance induced during the current sheet motion [7].

Assuming one dimensional model, with a planar current sheet perpendicular to the axis of the electrodes. This approximation is nearly true at high pressure [8], [9]. The change of momentum equation due to the force from (JxB).

$$\frac{dmv_z}{dt} = \frac{d}{dt}\left[f_m \rho \pi (b^2 - a^2) z(t) \frac{dz(t)}{dt}\right] = \int_a^b \frac{\mu (f_c I)^2 2\pi r\, dr}{2(2\pi r)^2} \quad (1)$$

Where a, and b are the radii of the anode and cathode respectively. ρ is the initial gas density of gas, μ is the permeability of the free space. f_m, and f_c are the snowplow mass swept up factor, and current factor respectively.

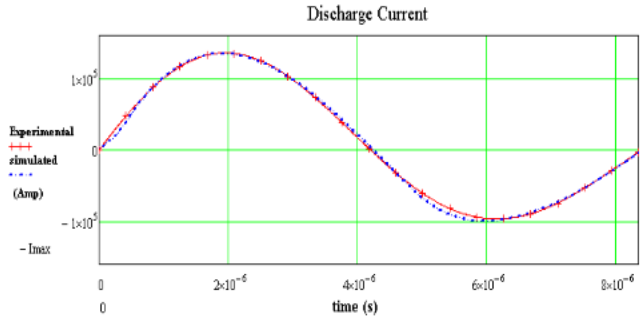

Fig. 2. The simulated current and the experimental current for deuterium at 40 mbar.

Therefore,

$$z(t)\frac{dz(t)}{dt}=\frac{\mu\ln(b/a)}{4\pi^2 f_m\rho(b^2-a^2)}\int(f_c I)^2 dt \quad (2)$$

Let $I_{norm}=I/I_o$, is the normalized current waveform, integrate to find the displacement of the current sheet z(t).

$$z(t)=\sqrt{2}U\left(\int\left(\int I_{norm}^2 dt'\right)dt\right)^{1/2} \quad (3)$$

Where,

$$U=\sqrt{\frac{\mu\ln(b/a)(f_c I_o)^2}{4\pi^2(f_m\rho)(b^2-a^2)}} \quad (4)$$

is the characteristic axial transient speed from which the axial speed will be,

$$\frac{dz}{dt}=\frac{U^2}{z}\int I_{norm}^2 dt \quad (5)$$

The theoretical current was calculated as sinusoidal wave modified by a damping function $I(t)=I_o e^{-\alpha t}\sin(\omega t)$, where α is the exponential damping coefficient ($R_o/2L_o$), and ω is the natural angular frequency ($\sqrt{\omega_d^2-\alpha^2}$); ω_d is the resonant radian frequency ($1/\sqrt{L_oC_o}$). The theoretical current was matched to the experimental current waveform by changing three factors; the frequency ω, the damping factor α, and amplitude I_o, see Fig. 2. The current waveform, the capacity for the capacitor, and the charged voltage supplied to the circuit were used to calculate the impedance of the circuit, these calculations can be obtained from SC analysis. Hence the axial position and axial speed can be calculated as a function of time.

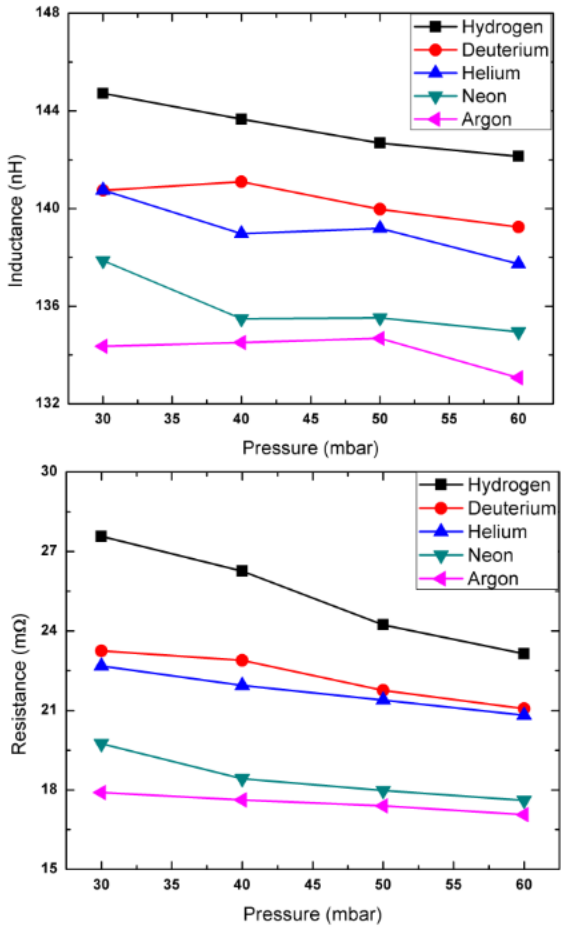

Fig. 3. The calculated resistance and inductance from the RLC model versus pressure.

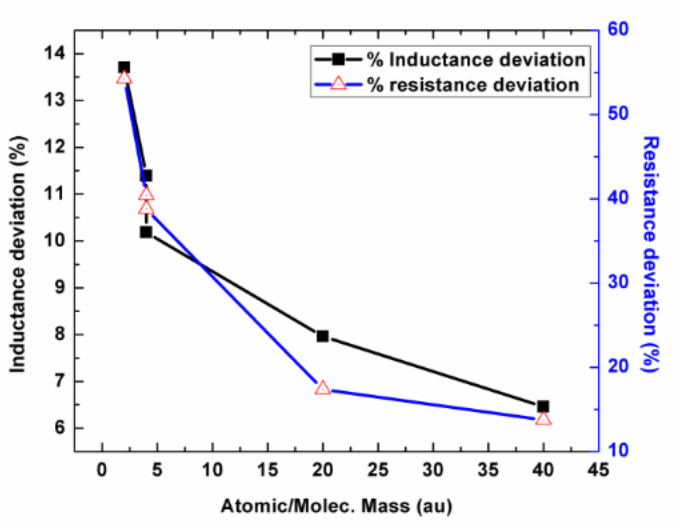

Fig. 4. HP inductance and resistance deviation versus the molecular mass of the used gas (at 60 mbar)

$$z(t)=\frac{U}{2\alpha(\alpha^2-\omega^2)}\begin{pmatrix}\alpha^4 e^{-2\alpha t}(1-\cos(2\omega t))\\+\alpha^2\omega^2 e^{-2\alpha t}(2+\cos(2\omega t))\\+2\alpha^3\omega e^{-2\alpha t}\sin(2\omega t)\\+\omega^4(e^{-2\alpha t}-1)-3\alpha^2\omega^2\\+2\alpha^3\omega^2 t+2\alpha\omega^4\end{pmatrix}^{1/2} \quad (6)$$

The axial speed will be,

$$\frac{dz(t)}{dt}=\frac{U^2}{4z(t)}\left(\frac{1-e^{-2\alpha t}}{\alpha}+\frac{\alpha e^{-2\alpha t}\cos(2\omega t)}{(\alpha^2+\omega^2)}-\frac{\omega e^{-2\alpha t}\sin(2\omega t)+\alpha}{(\alpha^2+\omega^2)}\right) \quad (7)$$

Therefore, the tube inductance due to the motion of current sheet can be determined as a function of the position.

$$L_p=\frac{\mu_o}{4\pi}\ln\left(\frac{b}{a}\right)Z(t) \quad (8)$$

The model was applied to previous experimental data from literature [8]-[10]. These works assumed approximate sinusoidal current waveform $I(t)=I_o\sin(\omega_n t)$ without the damping effect. Our damped model illustrated more precise matching to those experimental data in axial position and axial speed calculations.

V. Results

A. Experimental results

The SC test parameters were picked up from the KSU-DPF machine, for capacitor with C_o=12.5 μF, and V_o=17 kV, the reversal ratio f = 0.7974, and the periodic time T=7.852×10^{-6} s.

Therefore L_o=125nH, R_o=14.4 mΩ, I_o=153 kA. Then the Rogowski calibration factor (I_o/V_1) = 4.76×10^9 A/V, where V_1 is the first peak of Rogowski integrated signal corresponding to the current peak I_o.

The current waveforms from the HP tests were analyzed using RLC circuit analysis as stated before. The results show noticeable difference in inductance and resistance. This difference was dropping as the pressure increased Fig. 3, especially in light gases. The minimum calculated inductance and resistance recorded at 60 mbar argon were 133nH, and 17.1 mΩ respectively. The maximum values recorded at 30 mbar hydrogen were 145nH, and 27.6 mΩ.

This shows that the motion of current sheet is greater in light gases than in the heavy gases. The difference in between HP and SC results was considered as a deviation in L and R when using HP method as an approximation to find the static parameters. This deviation was calculated as a function of molecular mass of the working gas. Fig. 4 indicates the deviation percentage of resistance and inductance at 60mbar; it was found that the deviation percentage was inversely proportional to the molecular mass. At 60 mbar the deviation in calculated inductance varied from 14% for hydrogen to 6.5% for argon. The resistance deviation at the same conditions varied from 54% for hydrogen to 13.7% for argon.

B. Theoretical model results

Snowplow model was used to plot the axial position, speed and acceleration in the high pressure regime. Fig. 5 shows the axial parameters output. The solid lines express results from the damped sinusoidal current model and the dotted lines expresses the non-damped sinusoidal current model. These curves are corresponding to the first half cycle of the current waveforms. The model results indicated difference in axial position of about 30% and in speed of 15% between the two cases of current waveforms. Table A indicates the tube inductance (which is the SC inductance less the total inductance during plasma motion), corresponding axial position, and speed in various cases. The average axial speed was calculated for each gas on the range of the worked pressure. The average speed in the high pressure varies from 0.79 *cm/μs* in argon to 1.60 *cm/μs* in hydrogen.

VI. Conclusion

At the high pressure regime the KSU-DPF is operating at low shock wave speed; in such regime the coupling of energy provided to the plasma is predominantly through diffusive electrical discharge rather than electromagnetic piston-like. Nevertheless the data does indicate that there is downstream motion of the diffusive structure which we interpret as due to electromagnetic drive. Moreover the data for the average speed is found to be proportional to $(1/\rho)^{0.5}$ extending to the highest pressures which indicates that the speeds can be considered as electromagnetically driven even though we know the diffusive structure is electrically resistive. This interpretation is in a gross sense valid as evident from our analysis which shows in every case a significantly larger

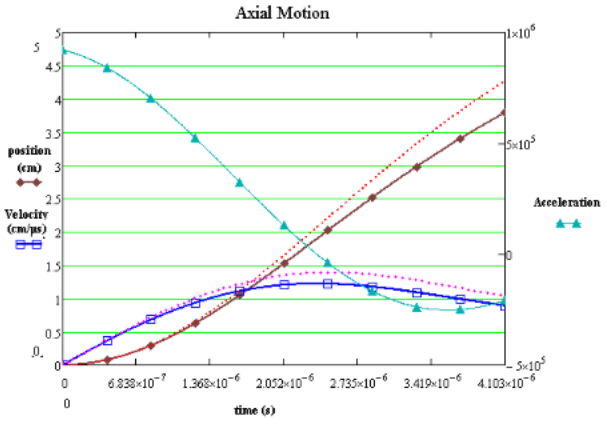

Fig. 5. Snowplow model using MathCAD dynamic sheet. Solid lines indicate the damped current model; the dotted lines indicate the sinusoidal current model. (data for neon at 40 mbar, 17 kV).

inductance and resistance from the HP tests when compared with the SC tests. We are therefore presenting this technique as a useful alternative method to the short circuit test in order to find out the static parameters for the machine. The induced error percentage due to the motion of current sheet was calculated using the approximate model. These results can be used as a reasonable first order correction to the values calculated with HP tests, and can be applied fairly on other machines with different geometries and energy scales. Under the high pressure regime, it was found that the speed of the current sheet is approximately one fifth the optimum speed in the normal working conditions. The deviation in L and R is proportional also to $(1/\rho)^{0.5}$ where ρ is the gas density.

TABLE A
Average axial position and axial speed values at different pressures

Gas	Pressure (mbar)	tube inductance Lp (nH)	Z (cm)	V (cm/μs)	Average speed (cm/μs)
Argon	60	7.36	2.83	0.70	0.79
	50	8.95	3.44	0.84	
	40	8.7	3.35	0.82	
	30	8.56	3.30	0.80	
Neon	60	9.32	3.58	0.87	0.96
	50	9.91	3.81	0.93	
	40	9.85	3.79	0.92	
	30	12.22	4.70	1.13	
Helium	60	12.20	4.70	1.13	1.25
	50	13.5	5.17	1.24	
	40	13.25	5.20	1.26	
	30	15.0	5.70	1.37	
Deuterium	60	13.39	5.15	1.23	1.32
	50	14.22	5.47	1.31	
	40	14.48	5.57	1.33	
	30	15.19	5.84	1.40	
Hydrogen	60	16.7	6.43	1.52	1.60
	50	17.09	6.58	1.55	
	40	17.7	6.80	1.60	
	30	19.18	7.38	1.732	

Finally it should be noted that although the use of the damped sinusoidal current in the snowplow equation of motion produces more accurate results than the use of an undamped sinusoidal current, but it is still an approximation when compared to the method of using the equation of motion coupled to the circuit equation. The coupled-equations method allows for the motion and the current to be derived as the two solutions of the two equation system. The nature of the problem is such that the current waveform is a damped sinusoid with non-linear time-varying damping factor as well as frequency; these are correctly incorporated into the point-by-point solutions as the coupled equations are numerically solved [1,11]. Nevertheless the use of a damped sinusoidal current in the equation of motion may still be used as a simpler alternative for analytical purposes.

REFERENCES

[1] S.H. Saw, S. Lee, F. Roy, P.L. Chong, V. Vengadeswaran, A.S.M. Sidik, Y.W. Leong and A. Singh, "In situ determination of the static inductance and resistance of a plasma focus capacitor bank," *Review of Scientific Instruments*, vol. 81, no. 5, pp. 053505-053505-4 2010.

[2] W A. Bernard, et al, "Scientific Status of Plasma Focus Research", J. Moscow Phys. vol .8, no. 2, pp. 93-170 1998.

[3] S. Lee, S. Saw, A. Abdou and H. Torreblanca, "Characterizing plasma focus Devices—Role of the static Inductance—Instability phase fitted by anomalous resistances," *J.Fusion Energy*, vol. 30, no. 4, pp. 277-282 2011.

[4] S S. Lee, Experiments With the ICTP-UM 3.3 kJ Plasma Fusion Facility, Spring College on Plasma Physics, International Centre for Theoretical Physics, Trieste, Italy, May 27–June 22 1991.

[5] D.A. Ward and J.L.T. Exon, "Using Rogowski coils for transient current measurements," *Engineering Science and Education Journal*, vol. 2, no. 3, pp. 105-113 1993.

[6] S. Lee, S. Saw, R. Rawat, P. Lee, R. Verma, A. Talebitaher, S. Hassan, A. Abdou, M. Ismail, A. Mohamed, H. Torreblanca, S. Al Hawat, M. Akel, P. Chong, F. Roy, A. Singh, D. Wong and K. Devi, "Measurement and processing of fast pulsed discharge current in plasma focus machines," *J.Fusion Energy*, pp. 1-7 2011.

[7] L.R.M. G, "A comment on the shape of the current sheet in a coaxial accelerator," *J.Phys.D*, vol. 11, no. 13, pp. 1911 1978. http://stacks.iop.org/0022-3727/11/i=13/a=013.

[8] M. Mathuthu, T. G. Zengeni, and A. V. Gholap, "Measurement of magnetic field and velocity profiles in 3.6 kJ United Nations University/ International Center for theoretical physics plasma focus," *Phys. Plasmas,* vol. 3, no. 12, pp. 4572–4576, 1996.

[9] S. Al-Hawat, "Axial velocity measurement of current sheath in a plasma focus device using a magnetic probe," *Plasma Science, IEEE Transactions on*, vol. 32, no. 2, pp. 764-769 2004.

[10] H. Bhuyan, S. R. Mohanty, N. K. Neog, S. Bujarbarua, and R. K. Rout "Magnetic probe measurements of current sheet dynamics in a coaxial plasma accelerator," *Measurement Science and Technology*, vol. 14, no. 10, pp. 1769 2003. http://stacks.iop.org/0957 0233/14/i=10/a=305.

[11] S Lee. Radiative Dense plasma Focus Computation Package (2011): RADPF www.plasmafocus.net ; www.intimal.edu.my/school/fas/UFLF/